

Containment Anchorage System Response to Pressures beyond Design

F. FANOUS, L. GREIMANN, W. WASSEF
Iowa State University, Ames, IA USA

ABSTRACT

A three-dimensional nonlinear finite element analysis of the anchorage system of an ice-condenser steel containment is presented. The finite element model consists of a one degree segment of the base-wall region. It includes a portion of the steel containment building, shield building, anchor bolt, anchorage system, reinforced concrete mat and soil foundation material.

1 INTRODUCTION

Recently, the Containment Technology Division of Sandia National Laboratories (SNL) has developed a method for predicting the performance of steel containment buildings under pressures that exceed the design values. To predict shell rupture, Sandia has suggested a failure criterion that is based on the ultimate strain properties of the material and adjusted by knockdown factors (Miller 1990). The knockdown factors account for differences between design and actual construction, sophistication of analysis methods, and variations in material property data.

A containment building fails to perform its function after a leak path is formed. Assuming that there are no pre-existing leak paths, a leak path can develop in a highly strained region of the containment. Among these leak paths is the containment-base connection. This paper summarizes the results of an analysis conducted for SNL to evaluate the performance of a typical ice-condenser steel containment anchorage system. The study was carried out using the ABAQUS general purpose finite element program (ABAQUS 1988).

2 CONTAINMENT DESCRIPTION

The steel containment that was analyzed in this work is a cylindrical steel structure fabricated with A516 Gr. 60 steel and is covered by a hemispherical dome. At the bottom there is a 1/4-in. thick steel base plate covered by two feet of concrete (see Fig. 1). The transition between the cylindrical plates forming the containment wall and the base plate is made through a knuckle plate welded to both. As shown in Fig. 1, this plate is formed from a 1/4 in. thick steel plate curved at an outer radius of 12 inches. The containment is held down by 180 pretensioned high strength bolts that resist the uplift forces generated by internal pressure or seismic events. These bolts are 2.5 inches in diameter and are preloaded to 25 ksi and embedded in a 12-foot-thick concrete

mat. The basemat is anchored into a rock foundation with several tie rods grouted into 10- to 15-foot deep holes. The steel containment vessel is surrounded by a 3-foot-thick reinforced concrete shield building.

3 FINITE ELEMENT MODEL

The symmetrical arrangement of the anchor bolts around the base of the containment vessel makes it possible to select a one-degree wedge extending from the center of one bolt to midway to the next bolt. The model includes portions of the containment vessel, shield building, anchor bolt, anchor plate, stiffener plates, reinforced concrete mat, and soil foundation material.

From the theory of plates and shells, bending is a local phenomenon whose effect diminishes at a distance of approximately $\pi \sqrt{rt}$, where r and t are the mean radius and the thickness of the cylindrical structure (Timoshenko 1959). With this consideration, the heights of the shield and containment building in the model were each limited to $3 \sqrt{rt}$. Figure 2 illustrates an outline of the finite element mesh used in the analysis. Eight-node solid elements (C3D8 in ABAQUS) were used to model the containment basemat and the shield building. Reinforcing bars, where provided, were modeled utilizing the rebar option in the ABAQUS program. The containment shell, base plate, knuckle plate, top and bottom rings as well as the vertical stiffener were modeled using 4-node shell elements (S4R5 in ABAQUS). The anchor bolt was idealized using beam elements (B31 in ABAQUS). The concrete-rock interface at the bottom of the basemat was idealized by compression-only springs (Spring1 in ABAQUS) whose stiffness was calculated by multiplying the foundation subgrade modulus times the tributary area for the spring. Tie rods between the rock and the concrete mat, were idealized by nonlinear tension-compression springs (Spring1 in ABAQUS). All interfaces between the steel plates and concrete elements were modeled using compression-only springs (Spring2 in ABAQUS) perpendicular to the plate. Frictional forces were neglected at the interface. Appropriate boundary conditions were imposed on the symmetry planes of the model. The model has 1935 elements and 4000 nodes.

Analytical modeling of a concrete structure with the finite element method requires consideration of several parameters that influence the predicted behavior of the structure. Bond idealization and shear transfer in cracked concrete were investigated utilizing small concrete finite element models (Fanous et. al. 1989). The analyses showed that the tension stiffening and shear retention employed in the ABAQUS program to idealize, respectively, bond and shear transfer parameters, respectively, gave satisfactory results and, hence, were selected to analyze the containment anchorage system.

4 LOADING AND SOLUTION STRATEGY

Following the application of the dead load and the bolt prestress load, an internal pressure was applied. Pressures were applied on both the containment shell and basemat. Meridional forces associated with the applied internal pressure were calculated and were applied upward at the top nodes of the containment shell. A sufficient number of iterations were allowed during the analysis until a converged solution was reached. Convergence in ABAQUS is attained when the maximum residual nodal forces are less than a user-specified tolerance, which is defined as a small fraction of the applied nodal forces.

The internal pressure was increased from zero to 30 psig in three steps. The load step size was then decreased to 5 psig up to a pressure of 40 psig. Beyond this pressure and up to a pressure of 70 psig, a load step size of 2 psig was used. This was further reduced to 1 psig and the analysis was carried to 73 psig. However, a singularity problem was encountered when the pressure was increased from 73 to 74 psig. The ABAQUS program indicated that the "plasticity algorithm did not converge at some nodes". The load step size was then decreased to 0.2 psig and the analysis was successfully performed to 73.8 psig.

Once again, no converged solution was obtained between 73.8 and 74 psig. The solution was restated from 73.8 psig using a pressure increment of 0.01 psig. However, the numerical problems were encountered as the pressure was increased to 74.13 psig. The load step size was decreased to 0.001 psig and the analysis was continued from a pressure of 74.12 psig. Converged solutions were reached as the pressure was increased to 74.123 psig; however, the plasticity convergence problem was again encountered beyond this pressure. Several unsuccessful attempts were made to continue the analysis beyond this pressure, but convergence could not be achieved.

5 RESULTS

5.1 Concrete Cracking

Fig. 3 illustrates the cracks along the symmetry plane through the anchor bolt in the basemat at a pressure of 74.123 psig. In the figure, the element is shown as cracked if a crack exists at, at least, one integration point (eight integration points/element). When cracks were formed at more than one integration point, crack orientation was determined by averaging the crack slopes. In the figures, the cracks in the first principal direction are shown as heavy lines while dashed lines were used to illustrate the cracks in the second principal direction. Elements that are cracked in the three principal directions are shaded in the figure.

Cracks first occurred in the concrete surrounding the anchor plate as the anchor pre-load was applied. As the pressure was applied, additional cracks formed in the vicinity of the anchorage system. Conical failure surfaces near the bottom ring and anchor plate started to form at 60 psig. All concrete surrounding the anchor bolt was cracked at 70 psig. At a pressure of 74.123 psig, a conical surface, with a slope of 40 degrees from the horizontal, extended from the outer edge of the bottom ring to Elev. 677' 9 3/8".

5.2 Component Loads

During the course of the analysis, about 94% of the applied load was transferred to the containment basemat through the bottom ring and the anchor bolt. The other 6% was transferred to the basemat through the top ring and the knuckle plate. The fraction of the load carried by the bottom ring decreased rapidly as cracks were formed in the concrete above the bottom ring. A larger share of the applied pressure was then transferred to the basemat through the anchor bolt. At 74.123 psig, the bottom ring carried about 40% of the anchor bolt load. The highest principal stress in the 3/8 in. fillet weld between the knuckle plate and the containment shell was 19,325 psi as the pressure reached 74.123 psig.

5.3 Steel Strains

The calculated strains in the knuckle, baseplate, anchor bolt, and the portion of the containment shell within the finite element model were well below the material ultimate strain. For example, the axial strain in the anchor bolt at 74.123 psig was 0.1% and the maximum inside surface strain in the containment shell at this pressure was 0.192%. The strain field in the shell was dominated by bending strain near the basemat-shell connection.

5.4 Deformed Shape

A deformed shape at a pressure of 74.123 psig for the concrete elements in the basemat in the vicinity of the anchor bolt is shown in Fig. 4. At low pressures, these deformations illustrated that the concrete cover above the top and bottom rings behave as short-deep cantilevers subjected to an upward force

(see Fig. 5). As the internal pressure was increased, the moments M_1 and M_2 (see Fig. 5) increased, resulting in tensile stress in the radial direction which caused vertical cracking on the left of the top and bottom rings. Similar behavior was also present in the region below the bottom ring. Notice that the discontinuity in the basemat caused by the embedded portion of the containment shell can be viewed as a built-in crack (see Fig. 5). The vertical cracks beneath the bottom ring were initiated by tensile stresses in the radial direction. These stresses were induced by the moment, M_3 , resulting from the upward pressure under the basemat and the weight of the shield building.

5.5 Possible Failure Modes

Several unsuccessful attempts were made to continue the analysis beyond 74.123 psig, but convergence could not be achieved. If the analysis had continued beyond 74.123 psig, enough cracks would probably have occurred to form a complete failure to occur in one of two possible modes: (1) formation of a complete failure cone above the anchor plate (brittle failure); or, (2) increase in the bolt strain with large deformation (ductile failure).

6 SUMMARY

A 3-D nonlinear finite element analysis of an ice-condenser steel containment anchorage system, which considers the parameters that affect this complex system, was performed. The model included a portion of the containment shell, knuckle plate, base plate, reinforced concrete mat, anchor bolt, anchorage system, soil foundation material, and a portion of the containment shield building. The results showed the early formation of conical failure surfaces within the concrete that are associated with the brittle failure mode. However, these surfaces were not completely developed to the top of the containment basemat. No high strains were recorded in the anchorage system or the containment shell. Hence, failure of the containment anchorage system could not be not predicted.

7 ACKNOWLEDGMENTS

This work was funded by Sandia National Laboratories through Contract No. 63-6130. The authors would like to express their appreciation to Dr. Brad Parks and Mr. D.B. Clauss from Sandia National Laboratories, and Dr. James Costello of U.S. Nuclear Regulatory Commission. The help of Mrs. Denise Wood for typing this paper is greatly appreciated.

8 REFERENCES

- Famous, F., Greimann, L.F and Gollapudi, V. (1989). Performance of Steel Containment Anchorage System During a Severe Accident, Transaction of the 10th International conference on Structural Mechanics in Reactor Technology, Vol. H, pp 1-6.
- Miller, J.D. (1990). Analysis of Shell-Rupture Failure Due to Hypothetical Elevated Temperature Pressurization of the Sequoyah Unit 1 Steel Containment Building, NUREG/CR-5405, SAND89-1650, Sandia National Laboratories, Albuquerque, NM.
- Timoshenko, S. and Woinowsky-Krieger, S. (1959). Theory of Plates and Shells, McGraw-Hill: New York.

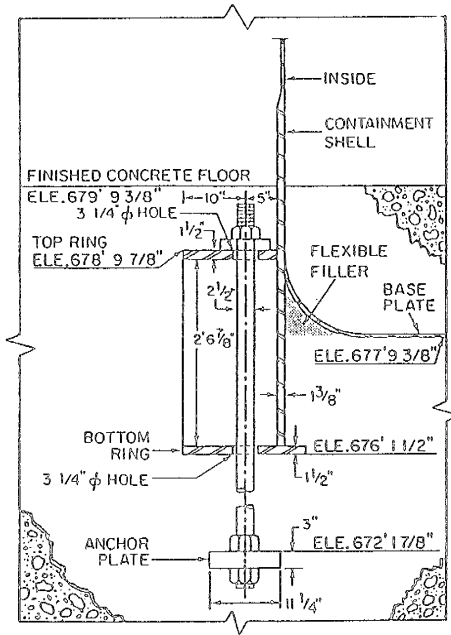


Fig. 1. Containment Anchorage System

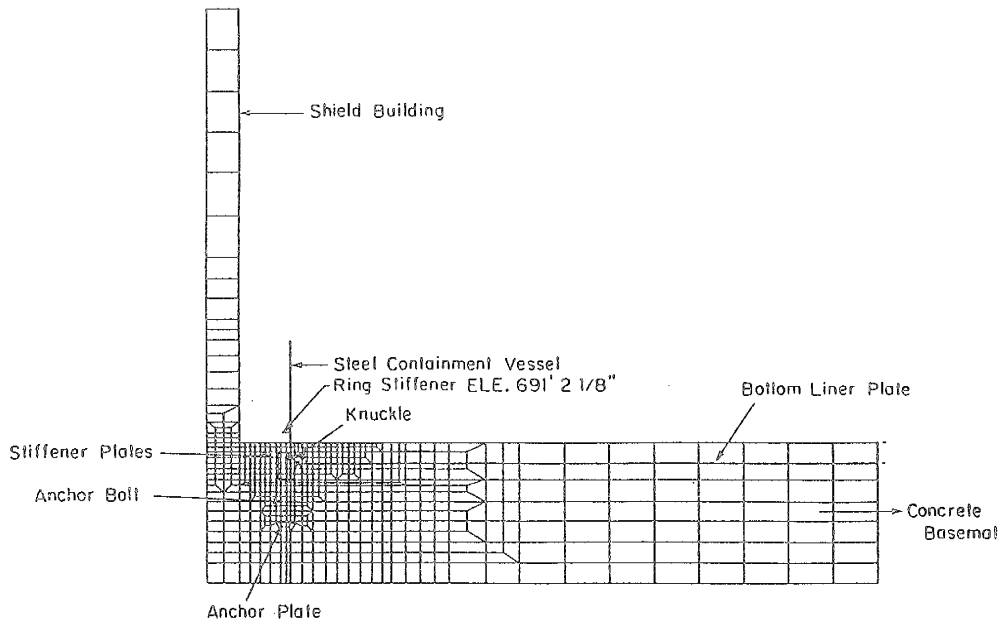


Fig. 2. Finite Element Model of the Containment Anchorage System

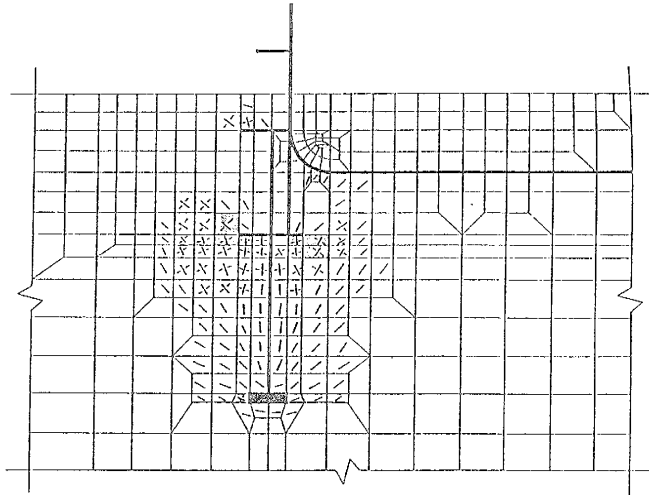


Fig. 3. Development of Cracks in the Containment Basemat at 74.123 psig

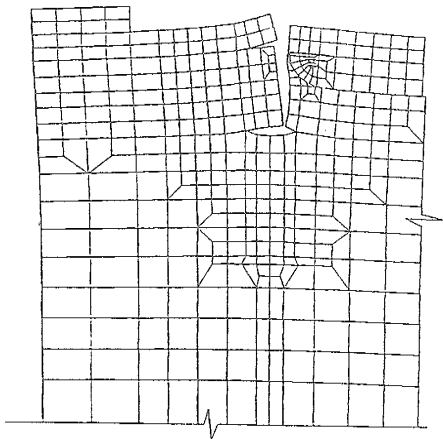


Fig. 4. Deformed Shape for the Containment Basemat in the Vicinity of the Anchorage System at 74.123 psig

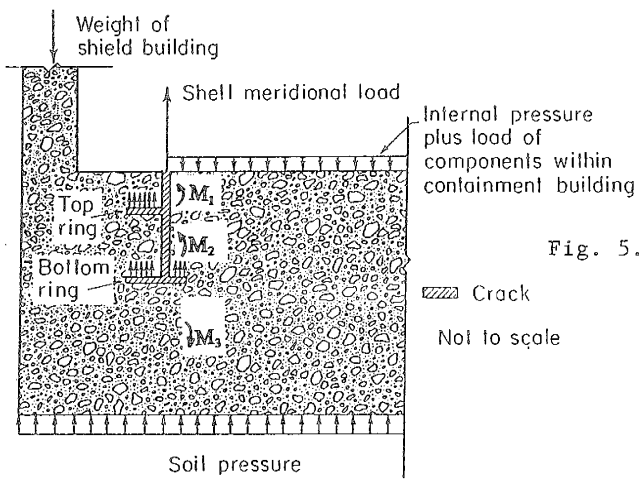


Fig. 5. Loads Acting on the Containment Basemat in the Vicinity of the Anchorage System (anchor bolt not shown)